# Molecular response properties from explicitly time-dependent configuration interaction methods

Pascal Krause, Tillmann Klamroth,[a] and Peter Saalfrank
*Theoretische Chemie, Institut für Chemie, Universität Potsdam, Karl-Liebknecht-Straße 24-25, D-14476 Potsdam, Germany*

(Received 28 March 2007; accepted 22 May 2007; published online 17 July 2007)

In this paper we report the calculation of molecular electric response properties with the help of explicitly time-dependent configuration interaction (TD-CI) methods. These methods have the advantage of being applicable (within the limitations of the time-dependent Schrödinger equation) to time-dependent perturbations of arbitrary shape and strength. Three variants are used to solve the time-dependent electronic Schrödinger equation, namely, the TD-CIS (inclusion of single excitations only), TD-CISD (inclusion of single and double excitations), and TD-CIS(D) (single excitations and perturbative treatment of double excitations) methods and applied for illustration to small molecules, $H_2$ and $H_2O$. In the calculation, slowly varying off-resonant electric fields are applied to the molecules and linear (polarizabilities) and nonlinear (hyperpolarizabilities, harmonic generation) response properties are determined from the time-dependent dipole moments. © *2007 American Institute of Physics*. [DOI: 10.1063/1.2749503]

## I. INTRODUCTION

The monitoring and control of electronic motion in atoms, molecules, and even adsorbates in real time became recently a dream come true.[1–4] This is particular due to the impressive advances in laser technology, which made few-cycle, attosecond (1 as$=10^{-18}$ s) laser pulses available.[5,6]

There is a tremendously enhanced interest on explicitly time-resolved electron dynamics also on the theory side, either "pure" or mixed with nuclear motion. In fact, after a few pioneering papers in the 1980s and 1990s,[7–9] the more recent, growing attention by theorists is evident from a certainly incomprehensive (and biased) list of papers.[10–27] In these papers, the focus is on the motion of electrons (or holes) on their natural time scales of a few femtoseconds down to the attosecond regime, where nuclear motion can often be neglected.

In our group, we have followed the direction of correlated many-electron dynamics using multideterminantal wave functions either derived from time-dependent configuration interaction[16,28,29] (TD-CI) or multiconfigurational time-dependent Hartree-Fock[30] (MCTDHF) methods. Both methods are systematically improvable towards the exact solution of the time-dependent electronic Schrödinger equation, for arbitrary time-dependent perturbations of the electronic system.

Time-dependent CI methods which explicitly included single excitations [TD-CIS and TD-CIS(D), see below] were recently applied to intramolecular charge transfer, induced by ultrashort laser pulses resonant with electronic transition energies.[29,31] It was found that electronic excitations with short, intense laser pulses are strongly influenced by linear and nonlinear molecular responses. Among other effects, the latter sometimes prevent the state-selective excitation of a molecule.

In this paper, we systematically address the possibility deriving linear and nonlinear electric response properties by solving the explicitly time-dependent electronic Schrödinger equation using TD-CI methods. For this purpose, nonresonant laser fields are employed and the time-dependent induced dipole moment is calculated from which, in turn, (static and dynamic) polarizabilities and hyperpolarizabilities can be determined. Traditionally, these properties are calculated from time-dependent perturbation theory, resulting in sum-over-states expressions without explicit time dependence if worked out in the frequency domain.[32–34] Various such and similar "stationary" techniques are implemented in standard quantum chemistry packages.[35] The explicitly time-dependent approach used here, on the other hand, has the advantage that not only the electronic motion can be followed in time, it is also nonperturbative (i.e., it contains formally all orders of perturbation theory), and it allows for arbitrary time dependence of the external field. As a long-term goal, the latter feature may be used to *control* the electric response of a molecule by shaping the laser pulse or a sequence of pulses.

The hydrogen molecule was chosen as a benchmark system for which TD-CI offers the possibility to improve both excitation level and basis set systematically towards the exact full-CI (FCI) solution at the basis set limit. For this purpose, TD-CI was extended to allow for the explicit inclusion of double excitations, and large basis sets were used to calculate linear and nonlinear response properties of $H_2$. The methods are further applied to the water molecule to demonstrate the performance of the methods in situations where no (numerically) exact reference exists.

The paper is organized as follows. In Sec. II we sketch

[a]Electronic mail: klamroth@uni-potsdam.de

 © 2007 American Institute of Physics

Downloaded 21 Nov 2007 to 141.89.199.236. Redistribution subject to AIP license or copyright; see http://jcp.aip.org/jcp/copyright.jsp

the TD-CI approaches used here, TD-CIS, TD-CISD, and TD-CIS(D). In Secs. III and IV we present the results, first for $H_2$ and then for $H_2O$. Section V summarizes the paper and gives an outlook for future work. We use atomic units throughout (with the exception that sometimes $\hbar$ is indicated for clarity), if not stated otherwise.

## II. THEORY

### A. CIS, CISD, and CIS(D)

In the following, we will use explicitly time-dependent variants of the well-known time-independent configuration interaction singles (CIS), configuration interaction singles doubles (CISD), and the configuration interaction singles (doubles) [CIS(D)] methods. In the time-dependent versions of these methods, termed TD-CIS (time-dependent CIS), TD-CIS(D), and TD-CISD, the electronic wave function is a linear combination of the Slater determinants containing single [TD-CIS and TD-CIS(D)] and double excitations (TD-CISD) out of the Hartree-Fock Slater determinant. In the time-dependent approach, the coefficients in front of the determinants are time dependent, in response to an external perturbation. Since the stationary methods are the basis for the time-dependent ones, and also to fix the notation, a brief summary of CIS, CISD, and CIS(D) is given.

As a single reference for all CI calculations we use the restricted Hartree-Fock ground state Slater determinant for an $N$-electron system,

$$|\Psi_0^{\mathrm{HF}}\rangle = \frac{1}{\sqrt{N!}}|(\psi_1\alpha),(\psi_1\beta),\ldots,(\psi_{N/2}\alpha),(\psi_{N/2}\beta)\rangle, \tag{1}$$

where there are $N/2$ spatial molecular orbitals (MOs), and $\psi_i$ are occupied with two electrons of opposite ($\alpha$ and $\beta$) spins. The spatial MOs are obtained from the spin- and field-free restricted Hartree-Fock equations $\hat{f}(\mathbf{r})\psi_n(\mathbf{r})=\varepsilon_n\psi_n(\mathbf{r})$, where $\hat{f}(\mathbf{r})$ is the one-electron Fock operator ($\mathbf{r}$=electron coordinate) and $\varepsilon_n$ the orbital energy of MO $n$.

#### 1. CIS

In CIS, the electronic wave function contains the HF Slater determinant $|\Psi_0^{\mathrm{HF}}\rangle$ and all singly excited determinants derived thereof. Singly excited determinants are derived from the HF ground state determinant by exciting an $\alpha$ electron from an occupied spatial MO $a$ to an unoccupied spatial MO $r(\Psi_a^r)$ or by exciting a $\beta$ electron ($\Psi_{\bar{a}}^{\bar{r}}$), respectively. Pure singlet and triplet spin states can be derived from these determinants by linear combination of $\Psi_a^r$ and $\Psi_{\bar{a}}^{\bar{r}}$. Here we are only interested in the singlet excited state manifold, where the singlet configuration state functions (CSFs) are, with the notation given in Ref. 36,

$${}^1\Psi_a^r = \frac{1}{\sqrt{2}}(\Psi_a^r + \Psi_{\bar{a}}^{\bar{r}}). \tag{2}$$

The electronic (singlet) wave functions are

$$\Psi_i = D_{0,i}\Psi_0^{\mathrm{HF}} + \sum_{a=L}^{N/2}\sum_{r=N/2+1}^{M} D_{a,i}^r\,{}^1\Psi_a^r. \tag{3}$$

$L$ denotes the lowest occupied orbital and $M$ the highest unoccupied orbital used to generate the excited determinants. The as yet time-independent coefficients $D$ are determined from diagonalizing the CIS Hamiltonian $\mathbf{H}^{\mathrm{CIS}}$:

$$\mathbf{H}^{\mathrm{CIS}}\mathbf{D}_i = E_i^{\mathrm{CIS}}\mathbf{D}_i. \tag{4}$$

In Eq. (4), $E_i^{\mathrm{CIS}}$ are the electronic excitation energies from the Hartree-Fock ground state with energy $E^{\mathrm{HF}}$, and $\mathbf{D}_i(D_{0,i},\{D_{a,i}^r\})$ is the state vector for state $i$. The matrix elements of $\mathbf{H}^{\mathrm{CIS}}$ are[36]

$$\langle\Psi_0^{\mathrm{HF}}|\hat{H}_0|{}^1\Psi_a^r\rangle = 0, \tag{5}$$

$$\langle{}^1\Psi_a^r|\hat{H}_0 - E^{\mathrm{HF}}|{}^1\Psi_b^s\rangle = (\varepsilon_r-\varepsilon_a)\delta_{rs}\delta_{ab} - \langle\psi_r\psi_b|\psi_s\psi_a\rangle + 2\langle\psi_r\psi_b|\psi_a\psi_s\rangle, \tag{6}$$

where $\hat{H}_0$ is the field-free electronic Hamiltonian,

$$\hat{H}_0 = -\tfrac{1}{2}\sum_{i=1}^{N}\boldsymbol{\nabla}_i^2 + \sum_{i=1}^{N}\sum_{j<i}^{N}\frac{1}{r_{ij}} - \sum_{A=1}^{N_A}\sum_{i=1}^{N}\frac{Z_A}{r_{iA}}. \tag{7}$$

Here and in Eq. (6), $N_A$ nuclei are assumed with nuclear charges $\{Z_A\}$ and position vectors $\{\mathbf{R}_A\}$,

$$r_{ij} = |\mathbf{r}_i - \mathbf{r}_j|,$$

$$r_{iA} = |\mathbf{r}_i - \mathbf{R}_A|,$$

and

$$\langle\psi_r\psi_b|\psi_a\psi_s\rangle = \int\int d\mathbf{r}_1 d\mathbf{r}_2\psi_r^*(\mathbf{r}_1)\psi_b^*(\mathbf{r}_2)r_{12}^{-1}\psi_s(\mathbf{r}_1)\psi_a(\mathbf{r}_2).$$

#### 2. CISD

For CISD, the electronic (singlet) wave functions contain, besides the HF Slater determinant (with coefficient $D_{0,i}$) and the singly excited determinants ${}^1\Psi_a^r$ (with coefficients $D_{a,i}^r$), also additional types of doubly excited CSFs,[36]

$$|{}^1\Psi_{aa}^{rr}\rangle = |\Psi_{a\bar{a}}^{r\bar{r}}\rangle,$$

$$|{}^1\Psi_{aa}^{r\acute{s}}\rangle = \frac{1}{\sqrt{2}}(|\Psi_{a\bar{a}}^{r\bar{s}}\rangle + |\Psi_{a\bar{a}}^{s\bar{r}}\rangle),$$

$$|{}^1\Psi_{ab}^{rr}\rangle = \frac{1}{\sqrt{2}}(|\Psi_{\bar{a}b}^{\bar{r}r}\rangle + |\Psi_{a\bar{b}}^{r\bar{r}}\rangle), \tag{8}$$

$$|{}^A\Psi_{ab}^{rs}\rangle = \frac{1}{\sqrt{12}}(2|\Psi_{ab}^{rs}\rangle + 2|\Psi_{\bar{a}\bar{b}}^{\bar{r}\bar{s}}\rangle - |\Psi_{\bar{a}b}^{\bar{s}r}\rangle + |\Psi_{\bar{a}b}^{\bar{r}s}\rangle + |\Psi_{a\bar{b}}^{r\bar{s}}\rangle - |\Psi_{a\bar{b}}^{s\bar{r}}\rangle),$$

$$|{}^B\Psi_{ab}^{rs}\rangle = \tfrac{1}{2}(|\Psi_{\bar{a}b}^{\bar{s}r}\rangle + |\Psi_{\bar{a}b}^{\bar{r}s}\rangle + |\Psi_{a\bar{b}}^{r\bar{s}}\rangle + |\Psi_{a\bar{b}}^{s\bar{r}}\rangle),$$

with coefficients $D_{ab,i}^{rs}$, ${}^AD_{ab,i}^{rs}$, and ${}^BD_{ab,i}^{rs}$.

Downloaded 21 Nov 2007 to 141.89.199.236. Redistribution subject to AIP license or copyright; see http://jcp.aip.org/jcp/copyright.jsp

The coefficients are obtained from diagonalizing the CISD matrix $\mathbf{H}^{\mathrm{CISD}}$. While the single excitations do not mix with the ground state according to Brillouin's theorem, Eq. (5), the doubly excited Slater determinants do. The CISD matrix elements, e.g., $\langle \Psi_0^{\mathrm{HF}} | \hat{H}_0 | {}^1\Psi_{aa}^{rr} \rangle$ or $\langle {}^B\Psi_{ab}^{rs} | \hat{H}_0 - E^{HF} | {}^B\Psi_{ab}^{rs} \rangle$, are evaluated by the Slater-Condon rules and are tabulated elsewhere.[36] Diagonalizing $\mathbf{H}^{\mathrm{CISD}}$ also gives the CISD excitation energies $E_i^{\mathrm{CISD}}$. Note that the CISD ground state is below the HF ground state because, other than CIS, the method accounts for electron correlation also for the ground state, not only for excited states.

#### 3. CIS(D)

The same is true for the CIS(D) method, in which double excitations are included as perturbative corrections to the ground and excited state energies obtained from CIS.[37] The size of the CI matrix is the same as in CIS, and the wave functions are still the CIS wave functions.

According to Ref. 37, one includes double excitations perturbatively as

$$E_i^{(D)} = -\tfrac{1}{4} \sum_{\mathrm{abrs}} \frac{(u_{\mathrm{ab},i}^{\mathrm{rs}})^2}{\Delta_{\mathrm{ab}}^{\mathrm{rs}} - E_i^{\mathrm{CIS}}} + \sum_{\mathrm{ar}} D_{\mathrm{a},i}^{\mathrm{r}} v_{\mathrm{a},i}^{\mathrm{r}}. \tag{9}$$

Here, the quantities $u_{\mathrm{ab},i}^{\mathrm{rs}}$ and $v_{\mathrm{a},i}^{r}$ are derived from two-electron integrals over spin orbitals, $\Delta_{\mathrm{ab}}^{\mathrm{rs}}$ from orbital energy differences, and $D_{\mathrm{a},i}^{\mathrm{r}}$ are derived from CI expansion coefficients as detailed elsewhere.[29,37] The corrected excitation energies are then

$$E_i^{\mathrm{CIS(D)}} = E_i^{\mathrm{CIS}} + E_i^{(\mathrm{D})}. \tag{10}$$

In CIS(D), the ground state energy is equal to the MP2 energy.[36]

### B. Time propagation

The laser-driven many-electron dynamics is treated by solving the time-dependent Schrödinger equation,

$$i \frac{\partial \Psi(t)}{\partial t} = \hat{H}(t) \Psi(t), \tag{11}$$

where

$$\hat{H}(t) = \hat{H}_0 - \hat{\boldsymbol{\mu}} \mathbf{F}(t) \tag{12}$$

is a time-dependent electronic Hamiltonian containing the dipole operator $\hat{\boldsymbol{\mu}} = -\Sigma_i^N \mathbf{r}_i + \Sigma_A^{N_A} Z_A \mathbf{R}_A$ and the electric field $\mathbf{F}(t)$.

The fields to be applied below are all chosen to be $\cos^2$ shaped, and can generally be written as

$$\mathbf{F}(t) = \mathbf{f}(t) \cos[\omega(t - t_p)], \tag{13}$$

$$\mathbf{f}(t) = \begin{cases} \mathbf{f}_0 \cos^2[(\pi/2\sigma)(t - t_p)] & \text{if } |t - t_p| < \sigma \\ \mathbf{0} & \text{else,} \end{cases} \tag{14}$$

where the pulse maximum $\mathbf{f}_0$ is reached at $t_p$, $\omega$ is the pulse frequency, and $\sigma$ the full width at half maximum (FWHM).

The time-dependent electronic wave function is expanded in the basis of the CI states as

$$\Psi(t) = \sum_i C_i(t) \Psi_i, \tag{15}$$

where the initial wave function at $t=0$ is the restricted Hartree-Fock (RHF) ground state, $\Psi_0^{\mathrm{HF}}$ for the TD-CIS and TD-CIS(D) methods, and $\Psi_0^{\mathrm{CISD}}$ in the case of TD-CISD. When the field is off, the propagation of the wave function is done quasianalytically as $\Psi(t+\Delta t) = \Sigma_i C_i(t) \exp(-\mathrm{i} E_i^{\mathrm{CI}} \Delta t) \Psi_i$. When the pulse is on, an operator splitting technique is used for the coefficient vector:[38]

$$\mathbf{C}(t + \Delta t) = \left[ \prod_{q=x,y,z} \mathbf{U}_q^{\dagger} e^{i F_q(t) \tilde{\boldsymbol{\mu}}_q \Delta t} \mathbf{U}_q \right] e^{-i \tilde{\mathbf{H}} \Delta t} \mathbf{C}(t). \tag{16}$$

Here, $\tilde{\mathbf{H}}$ is the Hamilton matrix in CI eigenstate basis, which we assume to be diagonal with the diagonal elements $\tilde{H}_{ii}$ being the CI excitation energies $E_i^{\mathrm{CI}}$. $\mathbf{U}_q$ $(q=x,y,z)$ are unitary matrices which transform from the CI eigenstate basis to a basis in which the dipole matrices $\tilde{\boldsymbol{\mu}}_q$ are diagonal.

In the calculations below, all singly (and doubly) excited singlet states are included to allow for all possible optical transitions from a singlet initial state. To calculate all the singlet excited states and the transition dipole moments, the one- and two-electron integrals in atomic orbital (AO) basis were taken from the GAMESS quantum chemistry program,[39] whereas the rest of the program was written from scratch. As an internal consistency check of the code, the RHF wave function and HF ground state properties were recalculated prior to the TD-CI run.

## III. THE $H_2$ MOLECULE

### A. Stationary quantum chemistry

The first step in a TD-CI calculation is an ordinary, stationary CI calculation. For $H_2$, we choose the molecular axis parallel to the $z$ axis, and the nuclear distance is set to the experimental value of $R_{\mathrm{H-H}} = 1.401 a_0$ (Ref. 40) and fixed throughout. Correlation-consistent and augmented correlation-consistent basis sets[41,42] have been used, which can be improved systematically. The smallest in this series is the correlation-consistent polarized valence double-zeta (cc-pVDZ) basis set, while the largest is the augmented correlation-consistent polarized valence quintuple-zeta (aug-cc-pV5Z) basis set. In the augmented case, diffuse functions are added.[42] In the following, the number $\zeta$ in (aug-)cc-pV$\zeta$Z is called the cardinal number. The number of molecular orbitals, $K$, ranges from 10 for cc-pVDZ up to 160 for the aug-cc-pV5Z basis. The number of excited singlet states ranges from 10 CSFs for CIS/cc-pVDZ up to 12 880 CSFs for CISD/aug-cc-pV5Z.

The ground state of $H_2$ is of ${}^1\Sigma_g$ symmetry. The HF ground state energy $(=E_0^{\mathrm{CIS}})$ for the largest basis set (aug-cc-pV5Z) is $-1.133\,605\ E_{\mathrm{h}}$. The MP2 $(=E_0^{\mathrm{CIS(D)}})$ ground state energy is $-1.167\,347\ E_{\mathrm{h}}$ for the same basis, and the CISD ground state energy is $-1.174\,252\ E_{\mathrm{h}}$, which corresponds to a correlation energy of $-0.040\,647\ E_{\mathrm{h}}$. The CISD/aug-cc-pV5Z value is in very good agreement with the exact treatment of the hydrogen molecule by Kołos and Wołniewicz,[43] giving $-1.174\,474\,77\ E_{\mathrm{h}}$ as the ground state energy, which corresponds to a correlation energy [calculated as $E_0$(exact)

Downloaded 21 Nov 2007 to 141.89.199.236. Redistribution subject to AIP license or copyright; see http://jcp.aip.org/jcp/copyright.jsp

TABLE I. Shown are the $z$ components of the transition dipole moments of $H_2$ together with the corresponding excitation energies calculated by the CISD method with the different basis sets (cc-pV$\zeta$Z and aug-cc-pV$\zeta$Z). Independent calculations of the excitation energies with the ACES2 program give, for the aug-cc-pV$\zeta$Z basis sets, perfect agreement for $\zeta$=D, T, and Q, while for $\zeta$=5 a small discrepancy to our calculation (of about 1 mhartree) exists, for reasons which are not clear (Ref. 64). All values are given in atomic units ($ea_0$ or $E_h$).

| | cc-pVDZ | cc-pVTZ | cc-pVQZ | cc-V5Z | Expt.[a] |
|---|---|---|---|---|---|
| $\lvert\mu_{0,1;z}\rvert$ | 1.237 8 | 1.209 2 | 1.160 9 | 1.095 9 | ⋯ |
| $\omega_{0,1}$ | 0.511 194 | 0.496 139 | 0.487 765 | 0.477 994 | 0.411 225 |
| | aug-cc-PVDZ | aug-cc-pVTZ | aug-cc-pVQZ | aug-cc-pV5Z | "Exact"[b] |
| $\lvert\mu_{0,1;z}\rvert$ | 0.993 6 | 0.973 5 | 0.979 3 | 0.989 8 | ⋯ |
| $\omega_{0,1}$ | 0.464 880 | 0.467 860 | 0.468 290 | 0.469 766 | 0.468 731 |

[a]Reference 44.
[b]Reference 45.

$-E_0^{\mathrm{CISD}}$(aug-cc-pV5Z)] of −0.040 870 $E_h$. The CISD/aug-cc-pV5Z is thus only 6 meV above the exact ground state energy.

The first excited singlet state of $H_2$ is of $^1\Sigma_u$ symmetry. Since the hydrogen molecule is homonuclear (point group $D_{\infty h}$), the permanent dipole moments are zero: $\mu_{0,0;z}=\mu_{1,1;z}=0$ (where $\mu_{n,m;z}=\langle\Psi_n|\hat{\mu}_z|\Psi_m\rangle$). However, there is a reasonably large transition dipole moment along the symmetry axis $z$, i.e., $\mu_{0,1;z}\neq 0$. The excitation frequencies $\omega_{0,1}=(E_1-E_0)/\hbar$ and transition dipole moments $\mu_{0,1;z}$ between ground and first excited states, obtained with the cc-pV$\zeta$Z and aug-cc-pV$\zeta$Z basis sets, are tabulated in Table I. Higher excited states were also calculated and are shown, if needed, below.

### B. Resonant excitation with $\pi$ pulses

While not the major concern of this work, we first demonstrate the performance of the TD-CI method when so-called $\pi$ pulses of $\cos^2$ from, resonant with the $\Psi_0\rightarrow\Psi_1$ transition, are applied, i.e., $\omega=\omega_{0,1}$ in Eq. (13). The field is assumed to be polarized along $z$, i.e., $\mathbf{f}(t)=(0,0,f_z(t))$. $\pi$ pulses induce a population inversion in an ideal two-level system. For a single $\cos^2$ pulse, the condition for the field amplitude is $f_{0,z}=\pi\hbar/\sigma|\mu_{0,1;z}|$.

For illustration the TD-CISD/aug-cc-pVDZ method is used, with an excitation frequency $\omega_{0,1}=0.464\,880\ E_h$ (Table I). Depending on whether a "long" or a "short" $\pi$ pulse is used, one obtains a state-selective excitation from $\Psi_0$ to $\Psi_1$, or an electronic wave packet, i.e., a coherent superposition of excited states. This is illustrated in Fig. 1, showing in the upper panels the *induced dipole moment* along the $z$ axis, $\mu_z(t)$ for $\sigma=1000\hbar/E_h$ (long pulse) and $\sigma=50\hbar/E_h$ (short pulse). In the lower panels the populations $P_i=|C_i|^2$ after the pulse is off are shown for various electronic states $\Psi_i$, when the initial state was $\Psi_0$.

We note that for the long pulse a state-selective transition to $\Psi_1$ occurs, and the dipole moment differs from zero only during the pulse. We find that the induced dipole moment $\mu_z(t)$ lacks the field $F_z(t)$ by a phase shift $\pi/2$ behind (like a classical, driven oscillator). As a consequence, the $\mu_z(t)$ trajectory is a helix in $\mu_z$-$F_z$-$t$ space, propagating the $t$ axis, with ellipsoidal structures when projected on the $\mu_z$-$F_z$ plane (so-called *Kennlinie*, see below). This spiraling is more clearly seen for the short pulse (right). In this case, an electronic wave packet is created and as a consequence the dipole moment is oscillating even after the field is off.

### C. Nonresonant excitation: Response properties of $H_2$

#### 1. Linear response: Static polarizability

For the calculation of response properties we use *nonresonant* electric fields $\mathbf{F}(t)$. In one of the simplest cases—a static field with a small field amplitude oriented along $z$—the response is linear and the induced dipole moment is $\mu_z^{\mathrm{ind}}=\alpha_{zz}F_z$. In the general case, the induced dipole moment along a coordinate $q$ (=$x$, $y$, or $z$) is (by using the sum convention for repeated indices)

$$\mu_q^{\mathrm{ind}}=\alpha_{qq'}F_{q'}+\tfrac{1}{2}\beta_{qq'q''}F_{q'}F_{q''}+\tfrac{1}{6}\gamma_{qq'q''q'''}F_{q'}F_{q''}F_{q'''}+\text{higher terms}, \tag{17}$$

where $\alpha_{qq'}$, $\beta_{qq'q''}$, and $\gamma_{qq'q''q'''}$ are elements of the polarizability and the first and second hyperpolarizability tensors, respectively. These depend, in general, on frequencies of frequency-dependent fields, e.g., $\alpha_{qq'}(-\omega;\omega)$, $\beta_{qq'q''}(-2\omega;\omega,\omega)$, and $\gamma_{qq'q''q'''}(-3\omega;\omega,\omega,\omega)$.

To determine the static polarizability in a time-dependent context, we use $\cos^2$-shaped, time-dependent electric fields [Eq. (13)], with a frequency $\omega=0$. The width of this half-cycle pulse is chosen as $1000\hbar/E_h$, and a moderate field strength of $f_{0,z}=10^{-5}\ E_h/(ea_0)$ ($3.51\times10^6$ W/cm$^2$). Due to its finite duration, the "pulse" has a frequency distribution with FWHM of 0.00225 $E_h$. Thus, the static polarizability is calculated as a quasistatic polarizability, determined here from the induced dipole at the peak maximum, i.e., $\alpha_{zz}=\mu_z(t_p)/f_{0,z}$.

As $z$ is chosen to be parallel to the symmetry axis, the two independent components of the polarizability tensor, parallel and perpendicular, are $\alpha_\parallel=\alpha_{zz}$ and $\alpha_\perp=\alpha_{xx}=\alpha_{yy}$. $\alpha_\perp$ is calculated as $\alpha_\perp=\mu_q(t_p)/f_{0,q}$, with $q=x$ or $y$. Average polarizabilities are calculated as $\alpha_{\mathrm{av}}=(\alpha_\parallel+2\alpha_\perp)/3$. In Table II, we show $\alpha_\parallel$, $\alpha_\perp$, and $\alpha_{\mathrm{av}}$ for various TD-CI methods/basis sets and in comparison to values obtained from other sources, both experimental and theoretical.

In the upper part of the table, we compare our results obtained with TD-CISD/aug-cc-pVQZ with those obtained

Downloaded 21 Nov 2007 to 141.89.199.236. Redistribution subject to AIP license or copyright; see http://jcp.aip.org/jcp/copyright.jsp

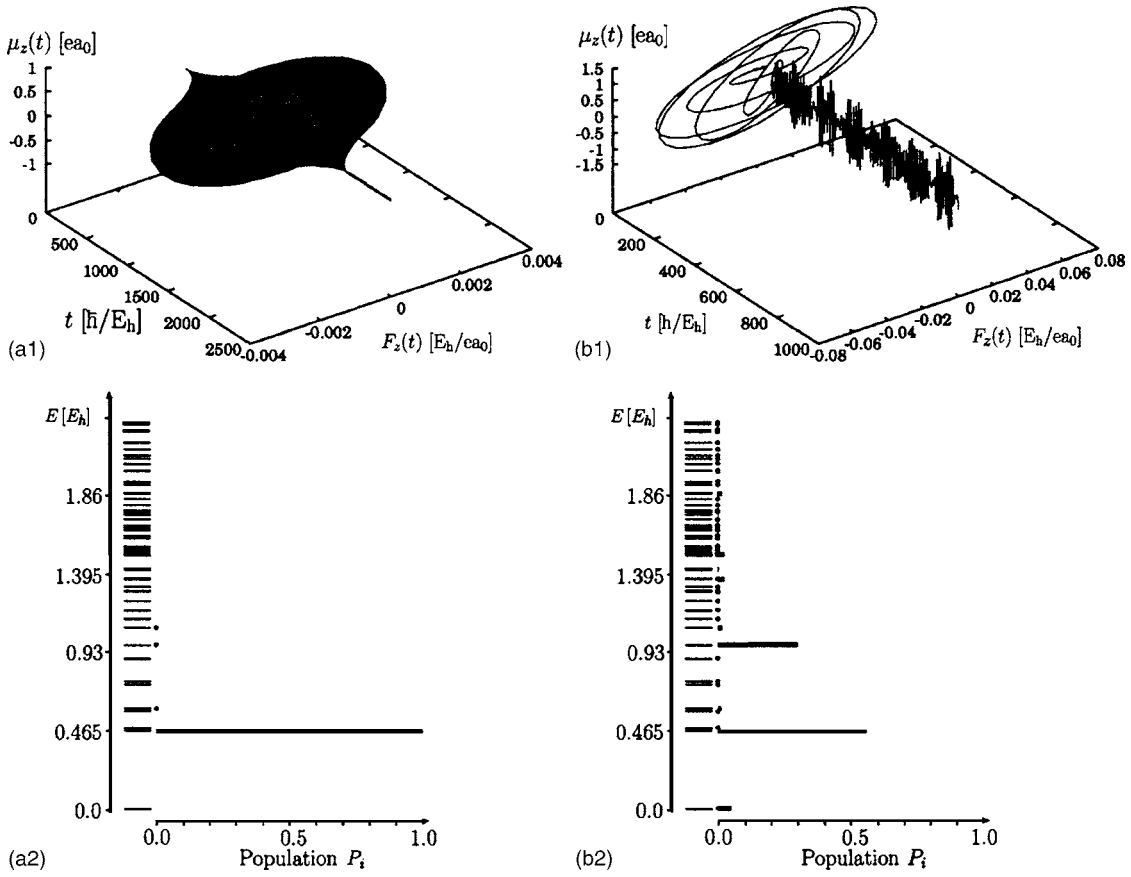


FIG. 1. In the upper panels shown are the dipole moments $\mu_z(t)$ as a function of the time $t$ and the field amplitude $F_z$ for an excitation with "long" [$\sigma=50\hbar/E_h$, (a1)] and "short" [$\sigma=1000\hbar/E_h$, (b1)] $\pi$ pulses. The lower panels [(a2) and (b2)] show the corresponding populations in various electronic states once the pulse is off. The TD-CISD method was employed with the aug-cc-pVDZ basis set and the laser frequency is chosen resonant with the $\Psi_0 \rightarrow \Psi_1$ transition.

with CISD/aug-cc-pVQZ from the GAUSSIAN03 (Ref. 35) program package, determined from the second derivative of the energy with respect to an electric field. We also compare to other theoretical and experimental values. First of all, the experimental values[49] of $\alpha_\parallel=6.303a_0^3$ and $\alpha_\perp=4.913a_0^3$ are in very good agreement with our quasistatic TD-CISD values, $6.3989a_0^3$ and $4.5845a_0^3$. The time-independent CISD/aug-cc-pVQZ polarizabilities obtained with the GAUSSIAN03 (Ref. 35) program package are in almost quantitative agreement with TD-CISD/aug-cc-pVQZ, i.e., $6.3997a_0^3$ and $4.5851a_0^3$

TABLE II. Listed are the quasistatic diagonal polarizability components of $H_2$ in comparison with experimental and other theoretical values. All values given are in $a_0^3$.

| | $\alpha_\parallel$ | $\alpha_\perp$ | $\alpha_{av}$ |
|---|---|---|---|
| TD-CISD/aug-cc-pVQZ | 6.3989 | 4.5845 | 5.1893 |
| CISD/aug-cc-pVQZ (Gaussian) | 6.3970 | 4.5749 | 5.1891 |
| Other theory | 6.370,[a]6.349[b] | 4.5841,[a]4.912[b] | 5.433,[b]5.53[c] |
| Expt. | 6.303[d] | 4.913[d] | 5.554[e] |
| TD-CISD/aug-cc-pVDZ | 6.5453 | 4.3512 | 5.0826 |
| aug-cc-pVTZ | 6.4073 | 4.6052 | 5.2059 |
| aug-cc-pVQZ | 6.3989 | 4.5845 | 5.1893 |
| aug-cc-pV5Z | 6.3964 | 4.5742 | 5.1816 |
| cc-pV5Z | 6.4097 | 3.8290 | 4.6892 |
| TD-CIS/aug-cc-pVQZ | 7.3720 | 4.9825 | 5.779 |
| TD-CIS(D)/aug-cc-pVQZ | 7.3209 | 4.9628 | 5.7488 |
| TD-CISD/aug-cc-pVQZ | 6.3989 | 4.5845 | 5.1893 |

[a]Reference 46.
[b]Reference 47.
[c]Reference 48 [measured/computed at a wavelength of 6328 Å (0.072 00 $E_h$)].
[d]Reference 49.
[e]Reference 50 [measured/computed at a wavelength of 6328 Å (0.072 00 $E_h$)].

Downloaded 21 Nov 2007 to 141.89.199.236. Redistribution subject to AIP license or copyright; see http://jcp.aip.org/jcp/copyright.jsp

for $\alpha_{\parallel}$ and $\alpha_{\perp}$, respectively. The agreement of TD-CISD/aug-cc-pVQZ with other theoretical studies of the static polarizability,[46,47] obtained at $R_{\mathrm{H-H}}=1.4a_0$, is also good. In Ref. 46, an exact variational method was used to solve the electronic Schrödinger equation in connection with perturbation theory for the polarizability. In Ref. 47, polarizabilities were obtained using the so-called double perturbation theory.

In the middle part of the table, we investigate the role of basis sets for the TD-CISD method. It is found that the $\alpha_{zz}$ values obtained with TD-CISD/aug-cc-pV$\zeta$Z are converged with $\zeta=Q$, up to three figures. The TD-CISD/cc-pV$\zeta$Z calculations show similar convergence behavior (not shown). While the TD-CISD/cc-pV5Z value of $\alpha_{\parallel}$ deviates from the TD-CISD/aug-cc-pV5Z result by only about 0.2%, the error for $\alpha_{\perp}$ is larger. For quantitative analysis, therefore, the augmented basis set should be used.

In the lowest part of the table, the method dependence is investigated for the aug-cc-pVQZ basis set (aug-cc-pV5Z is similar). It is found that the TD-CISD values are lower than TD-CIS and TD-CIS(D), the latter being only in moderate agreement with experimental and other theoretical values. This can be explained as follows. By including only single excitations explicitly as in TD-CIS and TD-CIS(D), a displaced electron leaves behind a localized hole in a previously occupied orbital, in this case the HOMO of $H_2$. Therefore, a second electron is also fixed and cannot respond to the displacement of the excited electron. In contrast, when double excitations are included, a second electron can move, for example, in the opposite direction to compensate for the total charge displacement and to reduce the value of the induced dipole.

### 2. Linear response: Dynamic polarizability

It is well known that the polarizability is frequency dependent and rises hyperbolically when approaching the excitation frequency for a transition $\Psi_0 \rightarrow \Psi_n$. This is evident, e.g., from time-dependent perturbation theory. The latter leads, for a field $F_z$ oriented along $z$, to the sum-over-states expression[51]

$$\alpha_{zz}(-\omega;\omega)=2\sum_{n\neq 0}\frac{\omega_{0,n}\mu_{0,n;z}^2}{\omega_{0,n}^2-\omega^2}. \tag{18}$$

Figure 2 shows five *Kennlinien* of $H_2$, obtained from five different carrier frequencies $\omega$ in Eq. (13), of $z$-polarized pulses with $f_{0,z}=1\times10^{-5}\ E_h/ea_0$ and $\sigma=1000\hbar/E_h$, when the TD-CISD/aug-cc-pVQZ method was applied.

For frequencies much smaller than the (first) excitation energy of 0.4649 $E_h$ (see Table I), we see straight lines $\mu_z(t)=\mu_z^{\mathrm{ind}}(t)\propto F_z(t)$. As the pulse frequency approaches the transition frequency, the line becomes steeper, indicating a larger value of the polarizability. Also seen for frequencies close to the transition energy is an increasing phase difference between the driving field and the electron oscillations, resulting in broadened lines. As shown in the previous section, a resonant excitation results in a rotating *Kennlinie* (see Fig. 1), which corresponds to a pole of the dynamic polarizability at the resonance frequency.

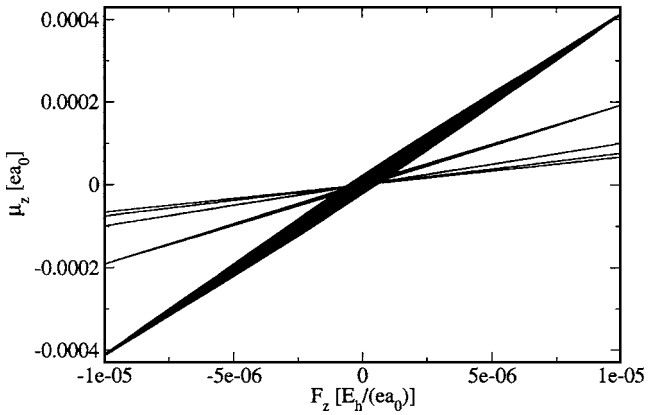


FIG. 2. Shown are the *Kennlinien*, $\mu_z(t)$ over $F_z(t)$, due to stimulation of $H_2$ with $\cos^2$ pulses with different carrier frequencies (0.10, 0.20, 0.30, 0.40, and 0.44 $E_h$, steeper lines correspond to larger frequencies). The TD-CISD/aug-cc-pVQZ calculations are done with $f_{0,z}=1\times10^{-5}\ E_h/ea_0$ and $\sigma=1000\hbar/E_h$.

The hyperbolical rise of the dynamic polarizability, as predicted from time-dependent perturbation theory, up to the transition frequency can be seen in Fig. 3. Plotted is $\alpha_{zz}$ as a function of the carrier frequency of the pulse. The $\alpha_{zz}(\omega)$ values were determined in the same manner like the quasistatic ones, as $\alpha_{zz}=\mu_z(t_p)/f_{0,z}$, at every carrier frequency. The frequency-dependent polarizabilities are calculated for the three TD-CI methods with the aug-cc-pVQZ basis set.

Obviously, the positions of the poles of the dynamic polarizability depend on the corresponding excitation energies and thus also on the underlying TD-CI method (see Table I). Other than that, comparing the TD-CI methods, the differences in the general behavior of the dynamic polarizabilities are small.

Our TD-CI data are compared with selected results of independent theoretical studies as cited in Refs. 52 and 53 in the inset of Fig. 3. These other studies have been carried out with perturbation theory using different wave-function-based

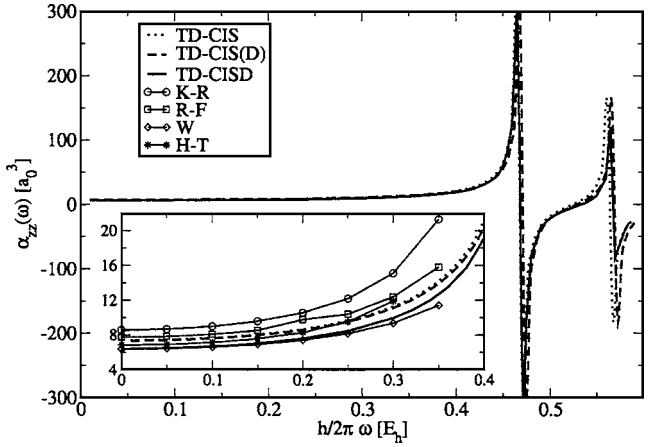


FIG. 3. Shown are the dynamic polarizabilities $\alpha_{zz}(\omega)$ of $H_2$ obtained from TD-CIS, TD-CIS(D), and TD-CISD calculations with the aug-cc-pVQZ basis set. The $\cos^2$-shaped laser pulse [Eq. (13)] has a maximum amplitude $f_{0,z}=1\times10^{-5}\ E_h/ea_0$ and a width $\sigma=1000\hbar/E_h$. Shown in the inset are the dynamic polarizabilities in comparison to variational calculations using different representations for the wave functions, as cited in Ref. 52: K-R=Kołos-Roothaan, R-F=Ransil-Fraga, W=Weinbaum, and H-T=Harris-Taylor.

Downloaded 21 Nov 2007 to 141.89.199.236. Redistribution subject to AIP license or copyright; see http://jcp.aip.org/jcp/copyright.jsp

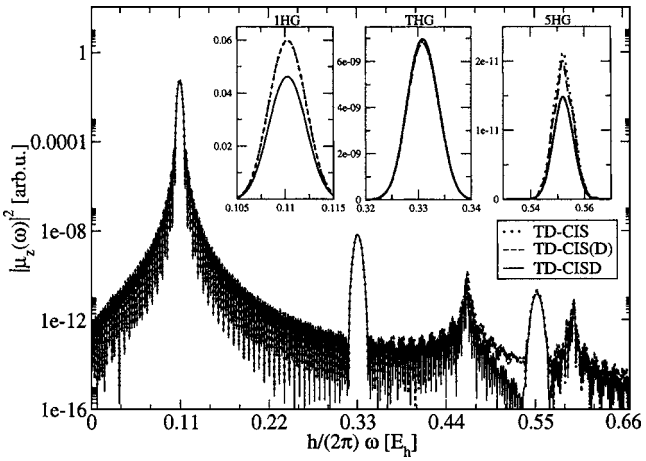


FIG. 4. Demonstrated is the harmonic generation for the different TD-CI methods. The frequency-dependent dipole moment squared is plotted on a logarithmic scale. The fundamental peak and the third and fifth harmonics are shown (nonlogarithmic and magnified) as insets. The TD-CIS, TD-CIS(D), and TD-CISD signals are calculated with the aug-cc-pVDZ basis set. The incident laser has a frequency of $\omega=0.1102\ E_h$ (3 eV), a maximum field amplitude of $f_{0,z}=0.007\ E_h/ea_0$, and a width $\sigma=1000\hbar/E_h$.

electronic structure models (see figure caption). Further theoretical studies of polarizabilities by using time-dependent density functional theory (TD-DFT) are given in Refs. 54 and 55. Note that, in contrast to TD-CISD, not all of the theoretical results shown in the inset are correct in the limit $\omega\rightarrow 0$. Apart from this, the differences between all methods shown are comparatively small, and the principle progression is well described.

### 3. Nonlinear response: Harmonic generation

Nonlinear responses due to hyperpolarizabilities are not directly observed in the time-dependent dipole moments for the cases considered above. They are automatically included, however, in our nonperturbative treatment and can be visualized by Fourier transformation of $\mu_q(t)$. As a prominent example we choose the generation of harmonics by short laser pulses. Molecules exposed to intense laser fields develop time-dependent dipole moments and emit multiples of the incident laser frequency.

In order to generate harmonics, which reveal linear and nonlinear dynamic polarizabilities, again laser pulses [Eq. (13)] with laser frequencies that are off resonant to electronic transitions are applied. To illustrate the generation of harmonics, the induced dipole moment was Fourier transformed from the time domain to the frequency domain according to $\mu_z(\omega)=\int\mu_z(t)e^{-i\omega t}dt$. As a measure for the harmonic signals, we use $|\mu_z(\omega)|^2$ which is plotted on a logarithmic scale over $\omega$.

As the molecular symmetry of $H_2$ implies a center of inversion, the generation of even harmonics is dipole forbidden. Let us first discuss the influence of the TD-CI method on the generation of harmonics. In Fig. 4 "spectra" of the odd harmonics of $H_2$ for all three different TD-CI methods are shown, obtained from $z$-polarized pulses [Eq. (13)] with $\sigma=1000\hbar/E_h$, $f_{0,z}=0.007\ E_h/(ea_0)$, and $\omega=0.1102\ E_h$ (3 eV). The aug-cc-pVDZ basis set was employed.

Besides the high-frequency oscillations, which arise from the Fourier transformation of a dipole moment $\mu_z(t)$ that was followed only for a finite time, in Fig. 4 the signals of the fundamental, the third, and the fifth harmonic are recognized. Harmonics higher than the fifth are not observed in our calculations when using the present AO basis.

The fundamental signal at $\omega$, the first harmonic generation (1HG), is governed by the dynamic polarizability $\alpha_{zz}(-\omega;\omega)$. The second largest peak is the third harmonic generation (THG) at $3\omega$, which is governed by the second hyperpolarizability element $\gamma_{zzzz}(-3\omega;\omega,\omega,\omega)$. The fifth harmonic generation (5HG) signal is determined by the fourth hyperpolarizability, and so on. For the TD-CISD method, with its more realistic polarizability (see Table II), the intensity of the fundamental peak is lower than for CIS and CIS(D). Differences in the THG peak are hardly visible. The sharp, additional peaks around 0.46 and 0.59 $E_h$ are due to electronic transitions to excited states, which have nonzero transition dipole moments for the applied laser polarization (compare with the poles of the dynamic polarizabilities in Fig. 3).

Qualitatively, no significant differences between the various CI levels are observed. Since the generation of harmonics is mainly a one-electron process,[56] the simultaneous excitation of two electrons as in TD-CISD is of minor importance. Only the fact that polarizabilities are described with higher accuracy by TD-CISD qualifies the much higher computational effort.

We also note that the dependence of harmonic generation on the basis sets has been addressed in some detail. It is found that the diffuse functions, which are added in the augmented basis sets, play an important role in the generation of harmonics. With the cc-pVDZ basis, for example, nearly no THG signal is found and larger cardinal numbers are needed to create a signal. The THG signals obtained with augmented basis sets are at least two times larger as those obtained with cc-pV$\zeta$Z bases, and their dependence on the cardinal number becomes smaller. In summary, it is important to use diffuse, large basis sets in order to reveal higher harmonics which are due to hyperpolarizabilities.

## IV. THE WATER MOLECULE

### A. Stationary quantum chemistry

The stationary electronic structure of $H_2O$ was determined with the cc-pV$\zeta$Z and aug-cc-pV$\zeta$Z ($\zeta$=D,T,Q) basis sets in conjunction with the CIS and CIS(D) methods. For CISD only the double-zeta basis sets, cc-pVDZ and aug-cc-pVDZ, were feasible. The point group of water is $C_{2v}$, i.e., in the chosen orientation the $z$ axis is the dipole axis and $x$ is perpendicular to the molecular plane. The geometry was set to the experimental values for the gaseous water molecule,[57] with a H–O bond length of $R_{O-H}=1.809a_0$ and a H–O–H bond angle of $\alpha_{HOH}=104.474°$. In the following, results of calculations with the aug-cc-pVDZ basis set are presented. The 10 electrons of $H_2O$ result, for the aug-cc-pVDZ basis set, in 181 singlet CSFs for CIS and CIS(D) and 16 471 CSFs for CISD.

Downloaded 21 Nov 2007 to 141.89.199.236. Redistribution subject to AIP license or copyright; see http://jcp.aip.org/jcp/copyright.jsp

TABLE III. Listed are the calculated diagonal polarizability elements in comparison to experimental data. All TD-CI calculations are done with the aug-cc-pVDZ basis set. All values are determined at the same frequency of 514.5 nm (0.08 86 $E_h$) and given in $a_0^3$. ($\alpha_{zz}$ could not be determined more accurately.)

| | TD-CIS | TD-CIS(D) | TD-CISD | CCSD[a] | Expt.[b] |
|---|---|---|---|---|---|
| $\alpha_{xx}$ | 8.317 | 9.356 | 6.777 | 9.72 | 9.546(+0.086) |
| $\alpha_{yy}$ | 10.592 | 11.525 | 8.032 | 10.18 | 10.314(±0.090) |
| $\alpha_{zz}$ | 9.4 | 10.5 | 7.2 | 9.87 | 9.906(±0.021) |
| $\alpha_{av}$ | 9.436 | 10.460 | 7.336 | 9.93 | 9.922 |

[a]Reference 61.
[b]Reference 60.

In this case the HF ground state energy is −76.041 426 $E_h$, the total MP2 [CIS(D)] ground state energy is −76.263 255 $E_h$, and the CISD ground state energy is −76.261 164 $E_h$. The excitation energies for $\Psi_0(\tilde{X}\,^1A_1) \rightarrow \Psi_1(\tilde{A}\,^1B_1)$, which is dominated by the HOMO-LUMO transition, are 0.319 048 $E_h$ for the CIS method, 0.256 357 $E_h$ for the CIS(D) method, and 0.404 147 $E_h$ for the CISD method. Experimentally, the first absorption band of water due to the (dissociative) $\tilde{A}\,^1B_1$ state is around 7.4 eV, or 0.272 $E_h$.[58,59] Hence, CISD greatly overestimates the excitation energy in this case, while CIS and, in particular, CIS(D) are in better agreement with experiment. To compare with other theory in Ref. 59, for example, the excitation energy was 8.64 eV (0.318 $E_h$) when calculated with CIS, employing a very good basis set, and under the Tamm-Dancoff approximation. TD-DFT response theory gave, with the same basis set and the B3LYP functional, a value of 6.83 eV (0.251 $E_h$).[59]

## B. Response properties of $H_2O$

### 1. Linear response: Polarizabilities

We first address the linear response of water, for which a TD-FCI calculation was not feasible. To determine the diagonal elements $\alpha_{qq}$ of the polarizability tensor, $x$-, $y$-, and $z$-polarized laser pulses are applied, and the relation $\mu_q^{\mathrm{ind}} = \alpha_{qq'} F_{q'}$ is used. Note that for $q=z$ in addition to the induced dipole moment, there is also a permanent dipole moment, $\mu_{0,0;z} = -0.78 e a_0$. The calculated polarizabilities are determined at the same frequency of 514.5 nm (0.088 558 $E_h$) as the experimental ones, according to Ref. 60, and with low field amplitudes of $1\times10^{-5}\ E_h/(ea_0)$ for the $\cos^2$-shaped pulses according to Eq. (13). The resulting polarizabilities calculated with the aug-cc-pVDZ basis set are listed in Table III and compared to literature values, both experimental and theoretical.

The experimental data of Ref. 60 are derived from the Raman spectrum of water vapor. The theoretical values we compare with in the table are coupled cluster calculations on the CCSD/d-aug-cc-pVTZ level of theory, taken from Ref. 61. In addition, in Ref. 62 a comparison of density functional theory with standard *ab initio* methods reports that the average static polarizability $\alpha_{av}$ ranges from $8.505 a_0^3$ (SCF), over $9.792 a_0^3$ (MP2), to $10.634 a_0^3$ (BLYP). In Ref. 55, $\alpha_{av}$ has also been calculated with TD-DFT methods using different exchange correlation functionals. For example, $\alpha_{av} = 10.53 a_0^3$ (TD-LDA) and $\alpha_{av} = 10.63 a_0^3$ (TD-BLYP), both at $\omega = 0$. As seen in Table III and the values just mentioned, our TD-CIS and TD-CIS(D) results are in good agreement with literature values. The TD-CISD values are too low, however, simply because for water the TD-CISD excitation energies are too large [see above and also the sum-over-states formula (18)]. This is most probably due to the fact that the electron correlation is described better for the ground state than for the electronic excited states dominated by a single excitation within the CISD method. For example, the absolute values of the excited state energies are comparable for CIS and CISD, but, as mentioned above, in CIS the ground state is uncorrelated, while the CISD ground state is and hence the CISD excitation energies are too large in $H_2O$.

It is also mentioned that the off-diagonal elements of the polarizability tensor could be determined similarly. For instance, by applying a pulse polarized along $y$, a dipole moment along $x$ is induced in linear response as $\mu_x^{\mathrm{ind}} = \alpha_{xy} F_y$. Dynamic polarizabilities could be determined by using $\omega \neq 0$ in Eq. (13).

### 2. Nonlinear response: Hyperpolarizability and harmonic generation

From the time-dependent dipole moment, it is also possible to determine hyperpolarizabilities. For example, by applying a pulse $F_y(t;\omega)$ polarized along $y$ and with carrier frequency $\omega$, the total dipole moment along the molecular symmetry axis $z$ is

$$\mu_z(t) \approx \mu_{0,0;z} + \alpha_{zy}(-\omega;\omega) F_y(t;\omega) + \tfrac{1}{2}\beta_{zyy}(-2\omega;\omega,\omega) F_y^2(t;\omega). \tag{19}$$

Since $\mu_{0,0;z}$ and $\alpha_{zy}(-\omega;\omega)$ are known, $\beta_{zyy}$ can be determined from a quadratic fit of $\mu_z(t)$. For TD-CIS/aug-cc-pVDZ with a laser frequency corresponding to $\hbar\omega = 1$ eV (0.036 75 $E_h$), a pulse duration of $\sigma = 1000\hbar/E_h$, and a maximum field amplitude of $f_{0,y} = 0.05\ E_h/(ea_0)$, one obtains $\beta_{zyy}(-2\omega;\omega,\omega) \approx 18.8 a_0^5$. The TD-CIS(D)/aug-cc-pVDZ value is $25.2 a_0^5$, and TD-CISD/aug-cc-pVDZ grossly underestimates $\beta_{zyy}$ with a value of about $8.4 a_0^5$. Other tensor elements can be obtained in similar ways. By computing the dipole component along $q$ and applying a field along $q'$, one obtains $\beta_{qq'q'}$, and by applying two perpendicular field components $q'$ and $q''$, we obtain $\beta_{qq'q''}$. Frequency-dependent quantities could be obtained from using pulses with different carrier frequencies, $\omega$ and $\omega'$.

In the fully time-dependent framework, however, these calculations are costly and would better be done with a sta-

Downloaded 21 Nov 2007 to 141.89.199.236. Redistribution subject to AIP license or copyright; see http://jcp.aip.org/jcp/copyright.jsp

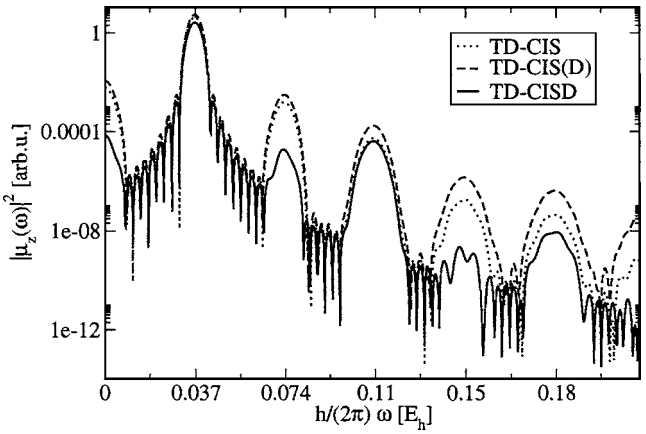


FIG. 5. Shown is the frequency-dependent dipole moment squared, $|\mu_z(\omega)|^2$, for the three TD-CI methods on a logarithmic scale. The calculations are done with the aug-cc-pVDZ basis set and the $\cos^2$ laser parameters are chosen to be $f_{0,z}=0.05\ E_h/ea_0$, $\omega=0.036\,75\ E_h$ (1 eV), $\sigma=1000\hbar/E_h$.

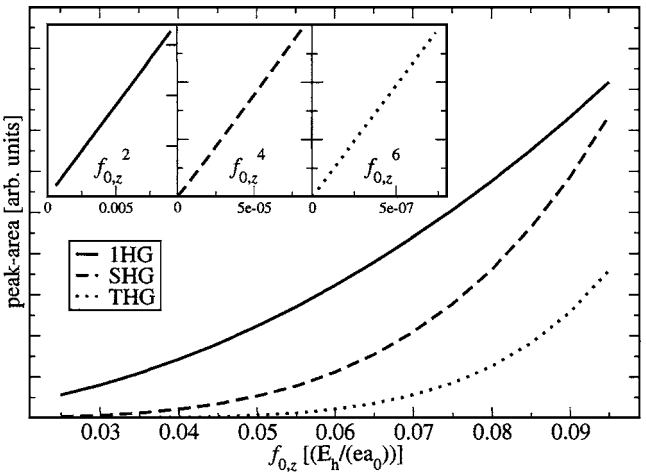


FIG. 6. Shown are the areas under the harmonic signals as a function of the maximum field amplitude $f_{0,z}$ calculated with the TD-CISD method. Solid line, area of the fundamental peak (1HG); dashed line, area of the second harmonic (SHG) peak (amplified by a factor of 1000); dotted line, area of the third harmonic (THG) peak (amplified by a factor of 50 000). The laser parameters are as follows: $z$ polarized, $\cos^2$ shaped, $\hbar\omega=0.036\,75\ E_h$ (1 eV), and $\sigma=1000\hbar/E_h$. Shown in the subfigures are the peak areas as a function of $f_{0,z}^2$, $f_{0,z}^4$, and $f_{0,z}^6$, respectively.

tionary method. A more interesting manifestation of nonlinear response, and better adapted to the time-dependent approach, is the process of harmonic generation after stimulation with a short laser pulse. For this purpose $z$-polarized laser pulses are applied. Odd and even harmonics are generated, because $H_2O$ has no center of inversion. Figure 5 shows the generation of the harmonics for all TD-CI methods.

These curves confirm the trend observed in the calculations on $H_2$ in the previous section. The values of the polarizability and the high-order hyperpolarizabilities for the TD-CISD method are always lower than those for TD-CIS and TD-CIS(D) (see above). Since the harmonics are due to polarizabilities and hyperpolarizabilities, the low intensities for TD-CISD reflect the fact that this method underestimates those. Interestingly, the even harmonics at $2\omega=0.074\ E_h$ and at $4\omega=0.15\ E_h$ are remarkably lower in intensity for TD-CISD than for TD-CIS and TD-CIS(D), while the fundamental and the odd harmonics are almost of the same intensity for every method.

To address basis set effects, harmonic signals for the cc-pVDZ and aug-cc-pVDZ basis sets of water were calculated with the TD-CISD method (not shown). It is found that diffuse functions are needed for a proper description, in particular, of the higher-order hyperpolarizabilities. For example, while the augmented basis set still resolves the fifth harmonic (at $0.18\ E_h$, see Fig. 5), the cc-pVDZ basis set does not. The 5HG signal is determined by the fourth-order hyperpolarizability.

In Fig. 6, the peak areas under the fundamental peak and the second and the third harmonics are plotted as a function of the maximum field amplitude, $f_{0,z}$. The peak areas under the signals are taken from the $|\mu_z(\omega)|^2$ curves obtained by TD-CISD/cc-pVDZ. Even without diffuse functions, the dependence of the peak area on the field intensity of the harmonics matches the expectations from perturbation theory.

More precisely, the 1HG signal is proportional to the square of the maximum field strength, $f_{0,z}^2$, i.e., proportional to the field intensity. The fundamental is due to induced dipole moment $\mu_q^{\rm ind}=\alpha_{qq'}(-\omega;\omega)F_{q'}(\omega)$ and hence the harmonic signal $|\mu_q(\omega)|^2$ proportional to the square of the field. Similarly, the SHG signal increases with $f_{0,z}^4$; here the first-order hyperpolarizability terms $\beta_{qq'q''}(-2\omega;\omega,\omega)F_{q'}(\omega)F_{q''}(\omega)$ contribute to the dipole moment and the scaling is quadratic in the intensity. Further, the THG signal, for which the induced dipole is determined from the second hyperpolarizability as $\gamma_{q,q',q'',q'''}(-3\omega;\omega,\omega)F_{q'}(\omega)F_{q''}(\omega)F_{q'''}(\omega)$, is proportional to $f_{0,z}^6$ and hence to the third power of the intensity. This behavior is indicated in the inset of Fig. 6, showing straight lines when the peak areas are plotted versus $f_{0,z}^2$, $f_{0,z}^4$, and $f_{0,z}^6$, respectively.

In order to give an impression of the computational effort here some technical details are given. The calculations have been carried out on dual-core Opteron 275 processors. For a total propagation time of $2500\hbar/E_h$ a TD-CIS(D)/aug-cc-pVQZ calculation requires 21 Mbytes memory and runs 7 min, while a TD-CISD/aug-cc-pVDZ calculation runs 4 days and requires 8 Gbytes memory.

## V. CONCLUSIONS AND OUTLOOK

In this paper, we applied the explicitly time-dependent TD-CI method for the calculation of the linear and nonlinear electric responses of $H_2$ and $H_2O$ molecules to an external, time-dependent perturbation. For the benchmark system $H_2$ it was shown that TD-CISD yields results for static and dynamic polarizabilities which are in quantitative agreement with high-level stationary calculations. For the $H_2O$ molecule it was demonstrated how to calculate polarizabilities and hyperpolarizabilities using explicitly time-dependent CI methods. Nonlinear response was also considered in the form of (higher) harmonics, calculated both for $H_2$ and $H_2O$.

We would like to reiterate the specific advantages of the explicitly time-dependent approach over a time-independent one. The first is for analysis, because information for specific

Downloaded 21 Nov 2007 to 141.89.199.236. Redistribution subject to AIP license or copyright; see http://jcp.aip.org/jcp/copyright.jsp

observables, such as the dipole moment, is available in real time. This gives insight into relevant time scales and the time order of individual processes driven by light. An even bigger advantage is that the molecular response for pulses with arbitrary time dependence is accessible, beyond perturbation theory. This, in turn, opens the perspective to turning the question around, i.e., to tune laser pulses or sequences of laser pulses such that a prespecified molecular response can be achieved, for instance, by use of optimal control theory.[31] The explicit time dependence can also be utilized for the inclusion of time-dependent "perturbations" other than an external field, e.g., the (classical) nuclear motion.

Last but not least, the time-dependent method has been demonstrated to be a valuable tool for calculating the linear and nonlinear responses of molecular systems, beyond perturbation theory. For this and other purposes, in future work we want to develop a TD-QCISD method, based on the quadratic configuration interaction singles doubles (QCISD) model, which is a powerful tool already in stationary quantum chemistry.[63] The more complete inclusion of higher-than-double excitations is another worthwhile goal. Finally, we wish to implement a continuum to describe ionization, e.g., in order to simulate also the generation of harmonics higher than those considered here.

## ACKNOWLEDGMENT

The authors gratefully acknowledge support of this work by the Deutsche Forschungsgemeinschaft through project Sa 547/6 (SPP-1145).

[1] M. Hentschel, R. Kienberger, C. Spielmann, G. A. Reider, N. Milosevic, T. Brabec, P. Corkum, U. Heinzmann, M. Drescher, and F. Krausz, Nature (London) **414**, 509 (2001).
[2] R. Kienberger, M. Hentschel, M. Uiberacker *et al.*, Science **297**, 1144 (2002).
[3] P. Bucksbaum, Nature (London) **421**, 593 (2003).
[4] A. Föhlisch, P. Feulner, F. Hennies, A. Fink, D. Menzel, D. Sanchez-Portal, P. Echenique, and W. Wurth, Nature (London) **436**, 7049 (2005).
[5] M. Drescher, M. Hentschel, R. Kienberger, M. Uiberacker, V. Yakovlev, A. Scrinzi, T. Westerwalbesloh, U. Kleineberg, U. Heinzmann, and F. Krausz, Nature (London) **419**, 803 (2002).
[6] G. G. Paulus, F. Lindner, H. Walther, A. Baltuška, E. Goulielmakis, M. Lezius, and F. Krausz, Phys. Rev. Lett. **91**, 253004 (2003).
[7] K. Kulander, Phys. Rev. A **36**, 2762 (1987).
[8] R. Grobe and J. H. Eberly, Phys. Rev. A **48**, 4664 (1993).
[9] M. Pindzola, P. Gavras, and T. Gorczyca, Phys. Rev. A **51**, 3999 (1995).
[10] H. Yu and A. Bandrauk, Phys. Rev. A **56**, 658 (1997).
[11] F. Remacle and R. Levine, J. Chem. Phys. **110**, 5089 (1999).
[12] F. Calvayrac, P.-G. Reinhard, E. Suraud, and C. Ullrich, Phys. Rep. **337**, 493 (2000).
[13] K. Harumiya, I. Kawata, H. Kono, and Y. Fujimura, J. Chem. Phys. **113**, 8953 (2000).
[14] H. Harumiya, H. Kono, and Y. Fujimura, Phys. Rev. A **66**, 043403 (2002).
[15] J. Breidbach and L. Cederbaum, J. Chem. Phys. **118**, 3983 (2003).
[16] T. Klamroth, Phys. Rev. B **68**, 245421 (2003).
[17] M. Suzuki and S. Mukamel, J. Chem. Phys. **119**, 4722 (2003).
[18] S. Laulan and H. Bachau, Phys. Rev. A **68**, 013409 (2003).
[19] F. Zanghellini, M. Kitzler, C. Fabian, T. Brabec, and A. Scrinzi, Laser Phys. **13**, 1064 (2003).
[20] T. Kato and H. Kono, Chem. Phys. Lett. **392**, 533 (2004).
[21] X. Chu and S. I. Chu, Phys. Rev. A **70**, 61402 (2004).
[22] G. Paramonov, Chem. Phys. Lett. **411**, 305 (2005).
[23] T. Burnus, M. Marques, and E. Gross, Phys. Rev. A **71**, 010501 (2005).
[24] X. S. Li, S. M. Smith, A. N. Markevitch, D. A. Romanov, R. J. Levis, and H. B. Schlegel, Phys. Chem. Chem. Phys. **7**, 233 (2005).
[25] I. Barth and J. Manz, Angew. Chem., Int. Ed. **45**, 2962 (2006).
[26] I. Barth, J. Manz, Y. Shigeta, and K. Yagi, J. Am. Chem. Soc. **128**, 7043 (2006).
[27] A. Castro, M. Marques, H. Appel, M. Oliveira, C. Rozzi, X. Andrade, F. Lorenzen, E. Gross, and A. Rubio, Phys. Status Solidi B **243**, 2465 (2006).
[28] P. Saalfrank, T. Klamroth, C. Huber, and P. Krause, Isr. J. Chem. **45**, 205 (2005).
[29] P. Krause, T. Klamroth, and P. Saalfrank, J. Chem. Phys. **123**, 074105 (2005).
[30] M. Nest, T. Klamroth, and P. Saalfrank, J. Chem. Phys. **122**, 124102 (2005).
[31] T. Klamroth, J. Chem. Phys. **124**, 144310 (2006).
[32] P. Craig and T. Thirunamachandran, *Molecular Quantum Electrodynamics* (Academic, New York, 1984).
[33] B. Gao, C. Pan, C.-R. Liu, and A. F. Starace, J. Opt. Soc. Am. B **7**, 622 (1990).
[34] M. Casida, C. Jamorski, K. Casida, and D. Salahub, J. Chem. Phys. **108**, 4439 (1998).
[35] M. J. Frisch, G. W. Trucks, H. B. Schlegel *et al.*, GAUSSIAN 03, Revision C.02, Gaussian, Inc., Wallingford, CT, 2004.
[36] A. Szabo and N. S. Ostlund, *Modern Quantum Chemistry*, 1st ed. (McGraw-Hill, New York, 1989).
[37] M. Head-Gordon, R. J. Rico, M. Oumi, and T. J. Lee, Chem. Phys. Lett. **219**, 21 (1994).
[38] A. D. Bandrauk, E. Aubanel, and S. Chelkowski, in *Femtosecond Chemistry*, edited by J. Manz and L. Wöste (Verlag Chemie, Weinheim., 1995), Vol. 2, Chap. 25, p. 731.
[39] M. W. Schmidt, K. K. Baldridge, J. A. Boatz *et al.*, J. Comput. Chem. **13**, 1347 (1993).
[40] G. Herzberg and L. L. Howe, Can. J. Phys. **37**, 636 (1959).
[41] T. H. Dunning, J. Chem. Phys. **90**, 1007 (1989).
[42] A. K. Wilson, T. van Mourik, and T. H. Dunning, J. Mol. Struct. **388**, 339 (1996).
[43] W. Kołos and L. Wolniewicz, J. Chem. Phys. **49**, 404 (1968).
[44] T. E. Sharp, At. Data **2**, 119 (1971).
[45] W. Kołos and L. Wolniewicz, J. Chem. Phys. **48**, 3672 (1968).
[46] W. Kołos and L. Wolniewicz, J. Chem. Phys. **46**, 1426 (1967).
[47] R. L. Wilkins and H. S. Taylor, J. Chem. Phys. **48**, 4934 (1968).
[48] N. J. Bridge and A. D. Buckingham, Proc. R. Soc. London, Ser. A **295**, 334 (1966).
[49] *Zahlenwerte und Funktionen*, Landolt-Börnstein, New Series, Vol. 1, Pt. 3, 1st ed. (Springer-Verlag, Berlin, 1951).
[50] G. A. Victor and A. Dalgarno, J. Chem. Phys. **50**, 2535 (1969).
[51] P. W. Atkins and R. S. Friedmann, *Molecular Quantum Mechanics*, 4th ed. (Oxford University Press, New York, 2005).
[52] G. A. Victor, J. C. Browne, and A. Dalgarno, Proc. Phys. Soc. London **92**, 42 (1967).
[53] T. Ando and A. Saika, J. Chem. Phys. **55**, 4203 (1971).
[54] S. J. A. van Gisbergen, J. G. Snijders, and E. J. Baerends, J. Chem. Phys. **103**, 9347 (1995).
[55] S. J. A. van Gisbergen, V. P. Osinga, O. V. Gritsenko, R. van Leeuwen, J. G. Snijders, and E. J. Baerends, J. Chem. Phys. **105**, 3142 (1996).
[56] P. Corkum, Phys. Rev. Lett. **71**, 1994 (1993).
[57] J. B. Hasted, in *Water a Comprehensive Treatise*, edited by F. Franks (Plenum, New York, 1972), Vol. 1, pp. 255–309.
[58] V. Engel, R. Schinke, and V. Staemmler, J. Chem. Phys. **88**, 129 (1988).
[59] S. Hirata and M. Head-Gordon, Chem. Phys. Lett. **314**, 291 (1999).
[60] W. F. Murphy, J. Chem. Phys. **67**, 5877 (1977).
[61] O. Christiansen, J. Gauss, and J. F. Stanton, Chem. Phys. Lett. **302**, 147 (1999).
[62] S. A. C. McDowell, R. D. Amos, and N. C. Handy, Chem. Phys. Lett. **235**, 1 (1995).
[63] J. A. Pople, M. Head-Gordon, and K. Raghavachari, J. Chem. Phys. **87**, 5968 (1987).
[64] W. Klopper (private communication).

Downloaded 21 Nov 2007 to 141.89.199.236. Redistribution subject to AIP license or copyright; see http://jcp.aip.org/jcp/copyright.jsp